JMBFS
Journal of Microbiology, Biotechnology and Food Sciences
International peer-reviewed scientific online journal

Published by Faculty of Biotechnology and Food Sciences

INFUSION CLONING, EXPRESSION AND PURIFICATION OF THE RECOMBINANT RITUXIMAB PRODUCED IN CHO CELLS

Chinnappa Reddy Veera[1, 2], *Partha Hazra*[2], *Kishore K. R. Tetala*[1*]

Address(es):
[1] Centre for Bioseparation Technology (CBST), Vellore Institute of Technology (VIT), Vellore, Tamil Nadu, India – 632014.
[2] Research and Development, Biocon Biologics Limited, Bangalore, Karnataka, India – 560099.

*Corresponding author: **:** kishore.tetala@gmail.com / kishore.tetala@vit.ac.in

https://doi.org/10.55251/jmbfs.12777

ARTICLE INFO

Received 8. 5. 2025
Revised 17. 11. 2025
Accepted 21. 11. 2025
Published 1. 12. 2025

Regular article

OPEN ACCESS

ABSTRACT

Rituximab is a crucial chimeric monoclonal antibody (mAb) used in the treatment of B-cell lymphomas, leukemia's, and certain autoimmune diseases. The process to identify the antibody gene, cloning and developing cell lines is a tedious, time consuming and costly process. Since, Rituximab effectively and specifically binds to CD20, it is important to develop faster and more affordable production method for this mAb. In this work, we have developed infusion based sequential cloning of light chain (LC) and heavy chain (HC) of Rituximab into a single expression vector followed by transfection of CHO-S cells. Fed-Batch analysis was performed to choose stable clone for the production of Rituximab. The Rituximab produced by the top two shortlisted clones was purified *via* affinity chromatography using an automated system with mAb Select Prism A resin. The resulting purified Rituximab was then characterized for size and charge variants using chromatographic methods, and its molecular weight (145 kDa) was confirmed through mass spectrometry studies.

Keywords: Rituximab, CHO-S cells, CE-SDS, SEC-HPLC, mass spectrometry

INTRODUCTION

Cancer forms are one of the leading causes of death worldwide, affecting people from all age groups and social status. WHO estimates that by 2030, the cancer burden will increase by 60 % globally **(World Health Organization, 2020)**. Various therapeutic approaches like surgical removal of the tumors, small molecules-based chemotherapy and radiotherapy have been used for ages and researched upon for the improvisation and decreasing of side-effects. The revolutionary new age therapeutics include the use of monoclonal antibodies (mAbs), immune checkpoint inhibitors, cell therapies and anti-cancer vaccines **(Falzone, Salomone, & Libra, 2018)**. This rapidly growing group of therapies are categorized as immunotherapies and is shown to have significant impact in the treatment of various cancers **(Lin et al., 2022; Lu et al., 2020; Singh et al., 2018a)**. Over the last 30 years, mAbs have garnered the attention as valuable therapeutics in various human diseases **(Jin et al., 2022; Singh et al., 2018a)**. mAbs are produced using hybridoma technology that was introduced by Köhler and Milstein in 1975 **(Köhler & Milstein, 1975)**. Since 1979, a series of murine mAbs were developed using this hybridoma technology and one of the first murine mAbs to be approved for human use was Muromomab. It was known to target the CD3 antigen on cytotoxic T-cells and was used to reduce the acute graft rejection episodes after transplantation of kidneys, liver, heart and combined transplants of kidney and pancreas. However, severe allergic reactions due to its murine origin has prevented its widespread use **(Todd & Brogden, 1989)**. Humanization of antibodies was pioneered by Greg Winter in 1988, which paved the way for the development of various therapeutic mAbs, including for cancer treatments **(Buss, Henderson, McFarlane, Shenton, & De Haan, 2012)**. Over the years, researchers have developed humanized mAbs to alleviate the side effects caused due to the murine components. This was done by replacing rodent sequences with human sequences, thus, resulting in chimeric, humanized and full human mAbs. In addition, the introduction of phage-display technology, use of single clonal cell selection and expansion and the availability of transgenic mice strains have further eased their production **(Buss et al., 2012)**. Adalimumab, the first full human mAb targeting tumor necrosis alpha (TNFα), was approved by the USFDA in 2002 for the treatment of autoimmune diseases like rheumatoid arthritis (RA) **(Buss et al., 2012; Singh et al., 2018b)**. Till 2022, the European Medicine Agency (EMA) or US Food and Drug Administration (FDA) has approved 111 mAbs for various clinical use. Importantly, 92 of them are chimeric, humanized and full human mAbs **(Kaplon & Reichert, 2021; Pierpont, Limper, & Richards, 2018; Walsh & Walsh, 2022)**. The successful application of immunoglobulin G (IgG)-based mAbs as therapeutics as well as other forms of antibodies (bi-specific antibodies, non-IgG mAbs, and antibody-drug conjugates), is being developed and used as alternative therapeutics for a broad range of cancers **(Falzone et al., 2018; Jin et al., 2022)**.

Rituximab is a chimeric mouse/human mAb approved by the FDA in 1997 to treat follicular lymphoma. It is composed of human Fc region and murine variable region against CD20 antigen of B-cells, leading to complement-dependent cytotoxicity, antibody-dependent cellular cytotoxicity (ADCC), and apoptosis of B cells. This has been successfully used for the treatment of diffuse large B-cell lymphoma, follicular lymphoma, chronic lymphocytic leukemia and rheumatoid arthritis **(Grillo-López, 2005; Maloney et al., 1997; Mishra, Singh, & Pritchard, 2011; Pierpont et al., 2018)**. Over the years, considering its immense importance as an established therapeutic, several biomanufacturers developed Rituximab and marketed it under different brand names, like Rixathon® (GP2013, Sandoz, Novartis), HLX01 (Shanghai Henlius Biotech, Inc.), Maball (Hetero biopharma) Reditux™ (Dr. Reddy's Laboratories), CT-P10 (Truxima®; Celltrion) and Ruxience® (Pfizer), **(Bennett, Qureshi, Singh, & Magwood, 2013; Coiffier, 2017; Sharman et al., 2020; Visser et al., 2013; Xu et al., 2019)**. While Rituximab is a chimeric anti-CD20 mAb (first generation), the second generation anti-CD20 mAbs are humanized and include Ocrelizumab, Obinutuzumab and Veltuzumab. Ofatumumab, a member of the newest generation of anti-CD20 mAbs, is a full-human mAb **(Du, Mills, & Mao-Draayer, 2017)**. Various clinical trials have been done with Ocrelizumab and Ofatumumab for the treatment of autoimmune disorders like RA or multiple sclerosis (MS; relapsing or progressive form) or systemic lupus erythematosus (SLE), along with Rituximab **(Margoni, Preziosa, Filippi, & Rocca, 2022; Sellebjerg, Blinkenberg, & Sorensen, 2020)**.

In this present study, a novel stable clone of CHO-S™ cells to express Rituximab was developed by cloning light chain (LC) and heavy chain (HC) into a pCHO 1.0 vector using an infusion cloning kit. The study discusses the process and results of molecular cloning, transfection and selection of a stable clone expressing Rituximab using various cell culture and analytical methods. Finally, this study provides a new stable clone that expresses Rituximab molecule.

MATERIALS AND METHODS

Cloning of Light chain and Heavy chain of Rituximab

The light chain (LC) and heavy chain (HC) of Rituximab were cloned into Freedom pCHO 1.0 vector (Thermo Fisher Scientific, USA) in a sequential manner using the 5X In-Fusion HD Enzyme Premix (Takara Bio USA Inc., USA). The HC and

LC genes of Rituximab sequences were obtained from drug bank (BTD00014, US patent 5736137) and were codon optimized for the expression in Chinese Hamster Overy (CHO) cells and synthesized. The genes were PCR amplified by using infusion primers from Sigma Aldrich as shown in Table S1, and Q5 DNA polymerase from New England Biolabs (NEB, USA).
The PCR products were run on agarose gel and checked for the presence of correctly sized amplicons (LC = 711 bp and HC = 1425 bp). The PCR products were purified from agarose gel using QIAprep gel extraction kit (Qiagen, GmbH). LC was cloned into Multiple Cloning Site 1 of Freedom™ pCHO 1.0 vector restriction, restriction-digested by EcoRV (NEB, USA) and PacI (NEB, USA). Once transformed, the colonies were screened for positive clones using colony PCR. One of the positive clones was subjected to sequencing to confirm the insert sequence. The resulting pCHO 1.0+LC clone was then restriction-digested with AvrII (NEB, USA) and BstZ17I (NEB, USA), and used for infusion cloning of HC into Multiple Cloning Site 2. Transformants were screened for positive clones by colony PCR. Two positive colonies pCHO1.0+LC+ HC, were then confirmed by plasmid miniprep (Qiagen, GmbH), and restriction digestion of the resulting plasmid DNA using various enzymes. One of the two colonies was used for transfection studies after sequence confirmation.

Transfection of CHO-S cells with linearized pCHO1.0+LC+HC

Plasmid consisting of Rituximab HC and LC genes, pCHO 1.0+LC+HC was isolated and confirmed by restriction-digestion and nucleotide sequencing. The plasmid was linearized using NruI-HF (NEB, USA) for efficient transfection into CHO-S™ cells. CHO-S™ cell bank (Thermo Fisher Scientific, USA) was thawed into CD Forti CHO™ medium (Thermo Fisher Scientific, USA) containing 8 mM Glutamine (Thermo Fisher Scientific, USA). The thawed cells were cultured in an Erlenmeyer flask at 37 ºC, 130-150 rpm in an orbital shaker. The CHO-S™ cells were sub-cultured for five passages before seeding the cells for transfection.
The transfection of CHO-S™ cells was done using Freedom™ CHO-S™ Kit (Thermo Fisher Scientific, USA), wherein FreeStyleMax™ (Thermo Fisher Scientific, USA) and Opti-SFM™ medium (Thermo Fisher Scientific, USA) were used for the preparation of the transfection mixture. The linearized plasmid of pCHO 1.0+LC+HC Clone#1 (named as Rituximab plasmid) was used for transfection. Two independent transfections were carried out with the Rituximab plasmid. A mock transfected control was maintained by carrying out the transfection without any plasmid in duplicates. After 48 h, the supernatant from Rituximab plasmid-transfected flasks was used to measure the antibody titer using Octet (PALL Forte-Bio, USA) **(Noy-Porat et al., 2021; Passariello et al., 2023; Swartz & Chen, 2018)**. The Rituximab-transfected and the mock-transfected flasks were used for further stable transfection selection.

Generation of a Stable Pool of Cells

Selection of stably transfected cells was done in two phases.

Phase I Selection

In the first phase of selection, post 48 h of transfection the cultures (cells) from the transfected flasks were seeded at 0.5×10^6 cells/mL density in 40 mL and 30 mL of chemically defined medium supplemented with L-Glutamine (Freedom™ CHO-S™ Kit User Guide) + Anti-clumping agent (1:100, Thermo Fisher Scientific, USA) hence forth called as medium-1. This medium-1 was used for static selection in 150 cm^2 T flasks and direct shaking in 125 mL Erlenmeyer flasks, respectively. The selection medium for phase I is a combination of Puromycin (Thermo Fisher Scientific, USA + Methotrexate (Sigma Aldrich, India) (10 µg/mL + 100 nM and 20µg/mL + 200 nM). Once the cells recovered from the applied selection pressure to >85% viability in 150 cm^2 T flasks, the cells were transferred to 125 mL Erlenmeyer flasks containing medium with the same selection pressure as earlier. Once the cells recovered to ~90% viability in shake flasks, stable pools were subjected to Selection phase-II and the remaining cells were banked with 10×10^6 cells/mL. The same was done for cells arising from both the transfections (transfected flasks).

Phase II Selection

Pools from Selection Phase-I were then subjected to the second phase of selection. The cell pools from phase I selection were seeded at 0.5×10^6 cells/mL density in 30 mL medium-1 in 125 mL Erlenmeyer flasks and incubated at 37 °C in an 8% CO_2 shaker incubator. The selection medium for phase II contained a combination of higher concentrations of Puromycin (Thermo Fisher Scientific, USA) + Methotrexate (Sigma Aldrich, India) (30 µg/mL + 500 nM and 50 µg/mL + 1000 nM) as compared to phase I selection medium. From the two transfections and two selection phases, eight different pools of stable cells (4 from each phase) were obtained and compared the expression.

Fed-Batch Evaluation of stable cell pools

The eight different pools of stable cells obtained after the two different phases of selection (Phases I and II) were grown in fed-batch for cell banking and productivity. For each of the 8 stable cell pools, 30 mL of medium-1 was seeded at a density of $0.5 – 0.6\times10^6$ cells/mL in a 125 mL Erlenmeyer flask. The flasks were incubated in an 8% CO_2 shaker incubator at 37 ºC, 130-150 rpm. Once the cell density crossed $>10\times10^6$/mL, temperature shift was done for the flasks from 37 °C to 33 °C. Feeds were added, and glucose levels were maintained at ~3%. Sampling was done from each flask for viable cell density and viability on different days. The level of Rituximab expression (titer measurement) in the cell supernatant was estimated using the Octet instrument (Protein-A binding method). Octet analysis is routinely used method to quantify recombinant protein (e.g., mAb) titer in CHO cell fed-batch supernatants. The clarified samples are loaded onto biosensors (e.g., Protein A for mAbs), where the protein binds to the immobilized ligand. The real-time wavelength shift, proportional to concentration, is measured. The Titer is then determined by comparing the binding response to a reference standard curve. This label-free, high-throughput method offers rapid, accurate, and direct quantification, which is crucial for process monitoring.

Viable cell-count determination and Viability calculation

To determine viable cell count, Vi-CELL XR Cell Viability Analyzer (Beckman Coulter, USA) was used. It is a video imaging system that automates the analysis of a wide variety of cell types using the principle of trypan blue dye exclusion protocol. Undiluted samples were used for a viable cell concentration range of $0.00 – 10.00\times10^6$ cells/mL. The sample with cell counts over 10.00×10^6 cells/mL was diluted in a 1:1 ratio using dilution buffer (phosphate buffer saline) provided by the Beckman Coulter reagent pack (Beckman Coulter, USA). These samples are further mixed with trypan blue, and the stained cells are measured and counted for viable cell concentration and % viability by Vi-Cell XR cell analyzer.

Single cell clone Selection

Based on the titer of the stable cell pools from each of the eight different flasks, **Flask 6** was shortlisted for single cell cloning using an automated single cell printer, F.Sight™ from Cytena. This instrument sorts of single cell into each well of a 96-well plate, leaving out the corner wells of a 96-well plate. The cells were then sorted into three separate 96-well plates with >95% confidence. For additional evidence of monoclonality, images of the cells were captured using Solentim Cell Metric® CLD (Advanced Instruments, USA) on 0, 1, 2 and 3rd day, respectively. At every stage, an arbitrary titer cut-off was set to shortlist the clones to be scaled up. Once the clonal cells reached confluency in 96-well plates, the cells were scaled up to 24-well plates, 6-well plates, and then seeded into 125 mL Erlenmeyer flasks directly in 30 mL medium.
Fed-Batch analysis was initiated for 12 shortlisted clones (out of 23 clones) to scale-up to 30 mL in SF125mL flask. The flasks were seeded with $0.5 – 0.6\times10^6$ cells/mL with 30 mL of medium-1 in a 125 mL Erlenmeyer. Once the cell density crossed $>10\times10^6$ cells/mL, the temperature was changed from 37 °C to 33 °C. Feeds were added, and glucose levels were maintained at ~3 % from day 3 till the day of harvest (day 14), respectively. Sampling was done from each flask for cell counts and Rituximab titer determination by Octet. Clones were shortlisted based on Rituximab titer. On day 14, all the samples were harvested and stored at -80 ºC for further analysis.
Another round of Fed-batch evaluation was done for the top 6 clones as described above. A similar analysis was carried out to shortlist the top clones. On day 14, all the samples were harvested and stored at -80 ºC for further analysis.

Small-scale purification and protein estimation

The purification of Rituximab from the stored harvests was done using liquid handling system (Tecan, Switzerland). Affinity robo column (Prism A resin, 0.6 mL - Cytiva) was equilibrated with 6 Column volumes of equilibration buffer containing Tris, EDTA, NaCl buffer at pH 7.0, followed by loading of harvests. The column was washed with wash I buffer (Tris, EDTA, NaCl buffer pH 7.0), Wash II buffer (Tris pH 7.0) and elution was done using Glycine, pH 3.0 buffer (Prism A, resin data sheet - Cytiva). Concentration of the purified protein was estimated using SoloVPE® System (Repligen, USA). The percentage recovery of the protein from each harvest was calculated, and the titer of Rituximab was estimated using Octet. All the parameters allowed the selection and banking of the two best clones.

Comparative physicochemical evaluation of expressed Rituximab.

The purified rituximab was processed for analysis and comparative evaluation.

Size exclusion Chromatography – high-performance liquid chromatography (SEC-HPLC)

Alliance HPLC system (Waters, USA) was used for SEC-HPLC analysis. Samples were injected into TSKgel® G3000SW$_{XL}$ HPLC Column (L×I.D. = 7.8 mm * 300 mm, Tosoh Bioscience LLC, USA). The mobile phase consists of sodium phosphate buffer (Sigma Aldrich, India). Rituximab samples were diluted to 5 mg/mL in mobile phase and injected to achieve 100 µg of total protein on the column. The run time was 60 min with the isocratic method at a flow rate of 0.3 mL/min. The column temperature was set at 25 °C (Goyal et al, 2021).

Capillary Electrophoresis Sodium Dodecyl Sulfate (CE-SDS) Analysis

CE-SDS analysis was executed in PA 800 Plus Capillary Electrophoresis system (AB Sciex LLC, USA) equipped with PDA detector. A bare fused-silica capillary (50 µm inner diameter, 30.2 cm total length and capillary aperture of 200 µm) was assembled into the capillary cartridge. For non-reduced conditions, samples were buffer exchanged, alkylated and incubated before analysis. In case of reduced conditions, samples were buffer exchanged, reduced and incubated before analysis. Both the samples were electrokinetically injected at 1 mg/mL, and separation was achieved at 17 kv for 30 min. The cartridge temperature was set at 25 °C (Goyal et al, 2021).

Cation exchange chromatography (CIEX)

Cation-exchange high-performance liquid chromatography (CIEX-HPLC) was performed using a Waters Alliance e2695 system (Waters, USA) with a UV detector. Samples were injected to ProPac^{TM} WCX-10 (4 x 250mm) analytical column (Thermo Scientific), and separation was achieved using sodium phosphate buffer. Rituximab samples were diluted to 1.5 mg/mL in mobile phase and injected to achieve 150 µg of total protein on the column. The run time was 75 min with a linear gradient at a flow rate of 0.9 mL/min. The column temperature was set at 25 °C (Goyal et al, 2021).

Intact Mass Analysis

Intact molecular masses for purified P1B10 and P11B9 products were determined using LC–MS analysis: LC (Thermo Vanquish UHPLC) was connected to a mass spectrometer (Thermo OrbiTrap Elite). Samples were de-salted by C4 reverse-phase (RP) chromatography column (Waters BEH 1.7 µm, 2.1 x 100 mm, 300 Å) over a shallow gradient in 30 min at a flow rate of 0.2 mL/min. 0.1% Trifluoroacetic acid in water (mobile phase A) and 0.08% Trifluoro acetic acid in acetonitrile (mobile phase B) were chosen as the mobile phases for this experiment. The mass spectrometer was run with a capillary voltage of +4.3 kV, Capillary temperature of 330 °C, S-Lens RF level of 60 %, and mass range of m/z 1500 - 4000 Da. A source temperature of 210 °C was used. The raw protein spectra were deconvoluted before evaluation using the BioPharma Finder software (Thermo). (Goyal et al, 2021).

RESULTS AND DISCUSSION

Cloning of Light chain and Heavy chain of Rituximab

Light chain (LC) and Heavy chain (HC) of Rituximab were amplified by PCR using infusion primers indicated in Table S1. Agarose gel electrophoresis revealed a single band at the expected size for both LC (711 bp) and HC (1425 bp) (Figure S1). Similarly, Freedom^{TM} pCHO 1.0 vector was digested with EcoRV and PacI, electrophoresed and purified for use in cloning of LC (Figure S2).
Infusion cloning technology was used for sequential cloning of LC and then HC into Freedom^{TM} pCHO 1.0 vector. Eight pCHO 1.0+LC colonies obtained on two separate Kanamycin-containing LB Agar plates (Plate A and B) were screened using colony PCR. Seven of the 8 colonies screened showed the presence of the LC insert in the vector (Figure 1A). The negative control and no-template control (NTC) did not show any amplification as expected, indicating the colony PCR is specific for LC. Plasmid DNA from colony 1 of pCHO 1.0+LC was further used for the infusion cloning of HC. The plasmid was digested using AvrII and BstZ17I, electrophoresed and purified (Figure S3). Transformation of the infusion ligation mix into DH5α resulted in multiple colonies, eight of which were screened using colony PCR. Five out of eight colonies for pCHO 1.0+LC+HC showed the presence of a PCR band for HC (Figure 1B), and 2 out of five were taken for plasmid miniprep.

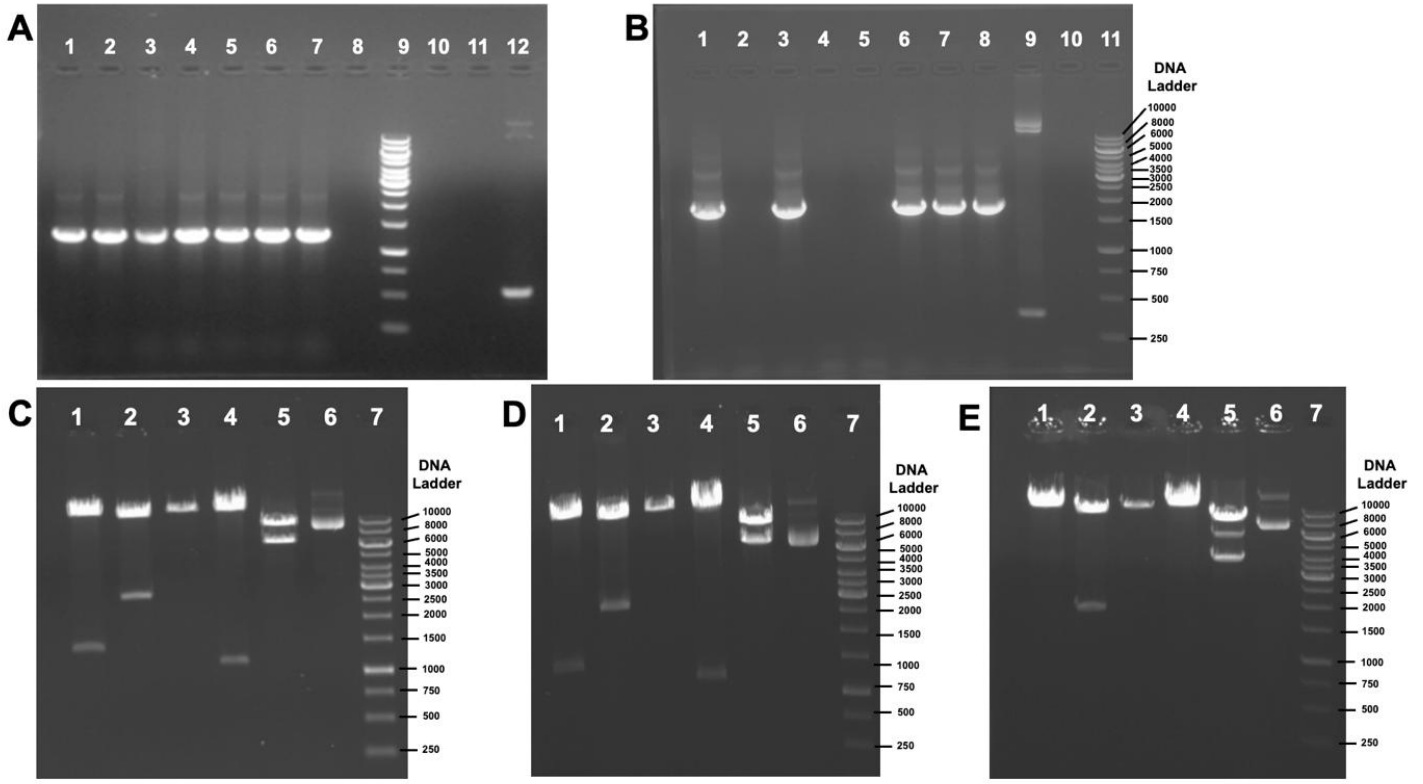

Figure 1 (A) Screening of pCHO 1.0 + LC clones using colony PCR. **Lanes 1-7:** PCR amplicon of ~1000 bp (pCHO 1.0 + LC); **Lane 9:** GeneRuler 1kb DNA Ladder; **Lane 10:** pCHO 1.0 (negative control); **Lane 11:** No template control; and **Lane 12:** Undigested pCHO 1.0 vector, **(B)** Screening of pCHO 1.0 + LC + HC clones using colony PCR. **Lanes 1-8:** PCR amplicon of ~1500 bp (pCHO 1.0 + LC + HC); **Lane 9:** Undigested pCHO 1.0 + LC vector; **Lane 10:** No template control; and **Lane 11:** GeneRuler 1kb DNA Ladder, **(C)** Confirmation by restriction digestion of pCHO 1.0+LC+HC clone 1, **(D)** Confirmation by restriction digestion of pCHO 1.0+LC+HC clone 3, and **(E)** Restriction digestion of pCHO 1.0 vector as control. **Lane 1:** Digestion with AvrII + BstZ17I; **Lane 2:** Digestion with BstZ17I + PacI; **Lane 3:** Digestion with NruI; **Lane 4:** Digestion with EcoRI; **Lane 5:** Digestion with KpnI + AvrII; **Lane 6:** Undigested plasmid of the corresponding clone; and **Lane 7:** GeneRuler 1kb DNA Ladder. (Note: Loading pattern in all the gels for **C, D,** and **E** were the same).

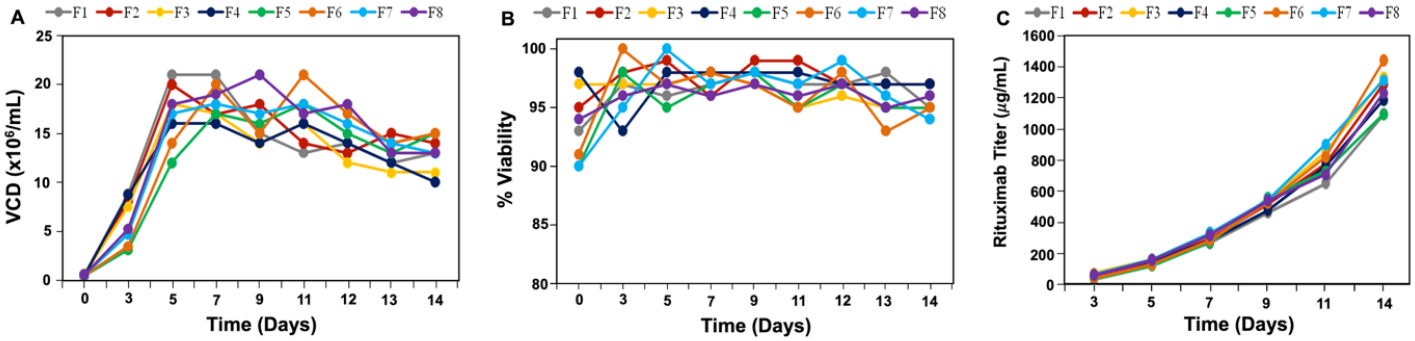

Figure 2 (A) Trend of Viable Cell Density (VCD) in the eight flasks (F1-F8), **(B)** Viability percentage (%) of cells in the eight flasks (F1-F8) in the tested days (0-14th day); **(C)** Production of Rituximab in µg/mL in the eight flasks (F1-F8) from 3rd – 14th Day.

Rituximab Clone Confirmation using Restriction Digestion

Cultures of colony 1 and 3 of pCHO 1.0+LC+HC were used for plasmid miniprep. The resulting plasmid was subjected to restriction enzyme digestion along with pCHO 1.0 vector as a control. The different restriction enzyme combinations and the expected band patterns are indicated in Table S2. Restriction digestion using different enzymes showed the expected band pattern in colony 1 and 3 of pCHO 1.0+LC+HC (Figure 1C and 1D). The band patterns for pCHO 1.0 vector also adhered to the expected pattern (Figure 1E). Sequencing of the plasmid of colony 1 for LC and HC was performed and contig alignment was performed using the Contig Express module in Vector NTI. The results showed 100% sequence identity to the reference sequence. Hereafter, pCHO 1.0+LC+HC colony 1 will be referred as Rituximab clone and was further selected to carry the transfections of CHO-S cells after linearization.

Transfection of CHO-S cells with Rituximab plasmid

CHO cells are the preferred cell line for production of monoclonal antibodies and other biosimilars due to their ability to be stably transfected as compared to other mammalian cell lines **(Bolisetty, Tremml, Xu, & Khetan, 2020; Ryu et al., 2022; Zitzmann et al., 2018)**.
CHO-S™ cells were transfected in duplicates with Rituximab plasmid using Freedom™ CHO-S™ Kit. At 48 h post transfection, the supernatant from Rituximab plasmid-transfected flasks was used to measure the antibody concentration using Protein A-bound Octet sensors. The antibody titers measured after 48 h for Rituximab-transfected flasks were 3.9 µg/mL and 4.7 µg/mL. As expected, the supernatant from mock-transfected flasks did not show the presence of antibody as measured by Octet.

Stable cell pool selection and Octet analysis

Upon introduction of the gene of interest (GoI) by transfection, random integration of the DNA sequence into the cellular genome is preferred for stable expression of the GoI. To select cells carrying the integrated DNA copy in their genomes, selection pressure, like antibiotics and metabolites was added to the medium **(Bolisetty et al., 2020; Longo, Kavran, Kim, & Leahy, 2014; Ryu et al., 2022**). To carry out the selection of stably transfected cells, at 48 h post-transfection, cells from the two flasks transfected with Rituximab were transferred to 150 cm^2 T flasks or 125 mL Erlenmeyer flasks and subjected to two phases of selection using Puromycin and Methotrexate. Eight different stable cell pools were obtained from this study Table S3. Octet analysis of supernatants from all the stable cell pool flasks was performed, and the results for the same are listed in Table S3.

Fed-Batch analyses of stable cell pools

Once the stable cell pools were selected and banked, fed-batch analyses were carried out using the selected stable cell pools to seed flasks as described in Materials and Methods. Fed-Batch analyses allow for the selection of cell pools that show stable and high expression of the protein of interest over the duration of analysis **(Bolisetty et al., 2020)**. Viable cell density and % viability was measured followed by Octet analysis for titer estimation for all eight flasks. While the viable cell density in each flask was in the range of 11 x 10^6 cells/mL and 21×10^6 cells/mL post Day 5 (Figure 2A), the viability of the cells was observed to be between 93% and 100% (Figure 2B). Octet analysis showed that flask F6, the stable cell pool derived from Rituximab Transfection Flask 2 and selected with 10 µg/mL Puromycin + 100 nM Methotrexate in first phase and 50 µg/ml Puromycin + 1000 nM Methotrexate in the second phase, had the highest titer of Rituximab at Day 14 (shown in bold in Table S4) (Figure 2C).

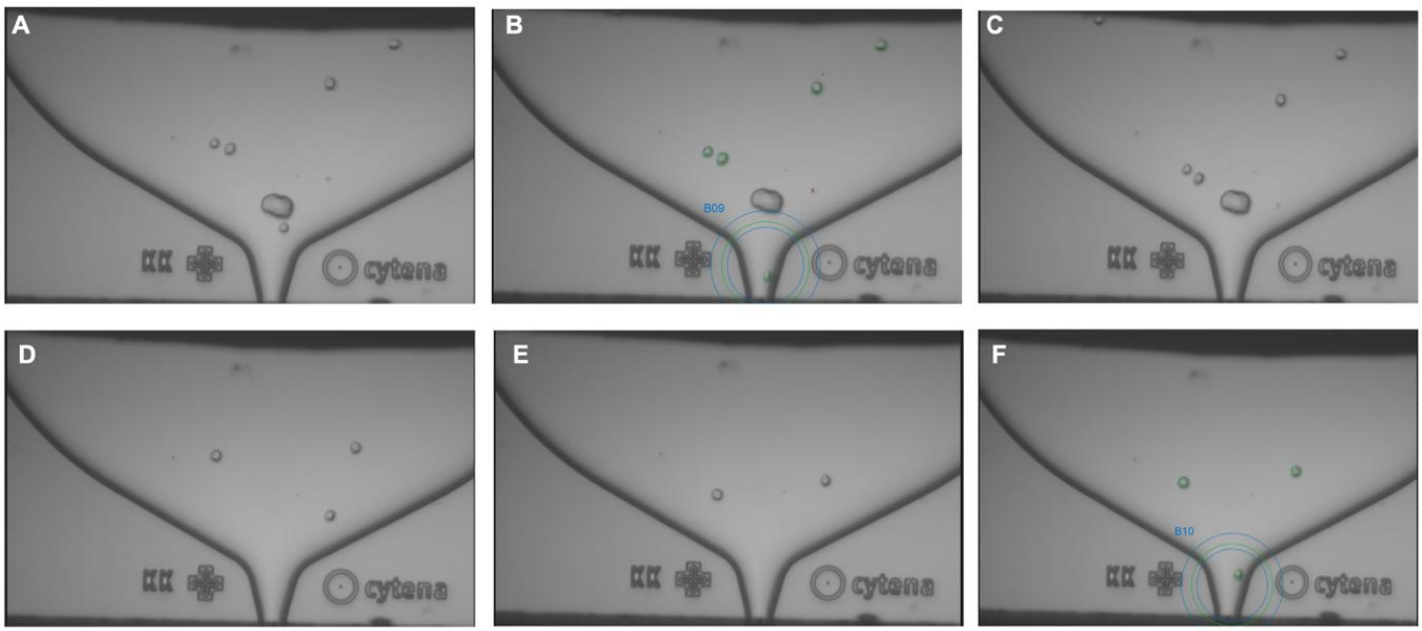

Figure 3 Microscope image of P1B10 single cell passage through F.Sight™ (Cytena) (**A**, **B** and **C**), and P2B9 single cell passage through F.Sight™ (Cytena) (**D**, **E** and **F**).

Single cell clone selection and Fed-Batch Analysis

Since the stable cell pool contains a heterogeneous population of cells, which have different levels of expression of the mAbs, variable number of copies integrated/cell, single cell clone selection allows sorting of cells into single colonies, which have a consistent expression level. This is one of the regulatory requirements to have the manufacturing cell bank population must originate from a single progenitor cell. This is a significant step for the selection of a consistently high-yield clone for commercial production of mAbs **(Bolisetty et al., 2020; Ryu et al., 2022)**. There are various methods like the limited dilution method **(Longo et al., 2014; Ryu et al., 2022)**, flow cytometry **(Yang, Zhang, Xiao, Li, & Wang, 2022)** and other advanced equipment like ClonePix, and microfluidics-based single cell sorting **(Yeh et al., 2020)** are being used for single cell cloning. F.Sight™ (Cytena) cell printer was used for the single cell clone selection from the Flask F6. This instrument is user-friendly to sort cells with proof of clonality through single cell images. The cell dispensing is gentle, with high seeding efficiency with low starting material requirements, providing a confidence of >95% for monoclonality. Various studies that employed this method have shown the instrument to be superior to other methods with accurate monoclonality and high recovery of clones **(Gross et al., 2021; Riba, Schoendube, Zimmermann, Koltay, & Zengerle, 2020; Scherzinger, Türk, & Aprile-Garcia, 2022; Vallone et al., 2020)**.
The images captured by Cytena F.Sight™ are shown in Figure 3 and 4. The images captured using Solentim Imager revealed the presence of a single cell on Day 0, followed by doubling of cell number on subsequent days (Days 1 and 2), which corroborated the monoclonal sorting done by Cytena F.Sight™. The monoclones were scaled-up from 96-well plates to 24-well plates, 6-well plates, and then seeded into 125 mL Erlenmeyer flasks and then the shortlisted clones were analyzed using Fed-Batch analysis. The overall selection criterion was based on titer at each step during scale-up. A Total of 12 clones were selected for Fed-Batch analysis and banked for future use (refer to Table S5 for sample ID). During Fed-Batch analysis, determination of Rituximab titres by Octet was done to shortlist the best clones out of the 12 clones (Table S5). 6 clones (P1B6, P1B10, P1G2, P2B5, P2B9 and P3E10) were selected for consistency studies in duplicates in a second run of Fed-Batch analysis followed by narrowing down the number of clones for further use (Table S6). Of the 6 screened clones for consistency, the top 2 clones (P1B10 and P2B9) were shortlisted based on their titer concentrations (837 and 1093 µg/L).

Small-scale purification and protein estimation

Small-scale purification of Rituximab from the two selected clones, P1B10 and P2B9, was done using Prism A (Protein A) resin. Table 1 depicts the stepwise yield of the protein for both the clones. The elute fraction was analyzed for the protein purity using Size exclusion chromatography – high performance liquid chromatography (SEC-HPLC). The results indicate that although P2B9 clone had a significant lower yield than P1B10 clone, its purity levels after Protein A chromatographic purification were better than clone P1B10.
Traditionally, Protein A resin is the most preferred resin for affinity purification of mAbs. However, in recent years researchers started to explore the use of Melon Gel™ resin **(Shukla, Radmall, & Chandrasekharan, 2023),** Mixed Mode Chromatography (MMC) resins (**Aoyama, Matsumoto, Mori, & Sota, 2022**) etc. as an alternative to protein A resins for the purification of IgG. The advantage of Melon Gel™ resin use is the use of negative chromatographic strategy under physiological conditions throughout the purification process thereby abrogating the requirement of harsh elution conditions for IgG. MMC uses multiple interaction modes (hydrophobic, hydrophilic, ionic etc.) to interact with IgG. However, MMC suffer from the requirement of long equilibration times, limited pH range, etc. Protein A resin strength is its high selectivity for IgG but suffers from the use harsh elution conditions that leads to leaching of Protein A moieties and also degradation of the mAbs purified **(Li, Dowd, Stewart, Burton, & Lowe, 1998)**.

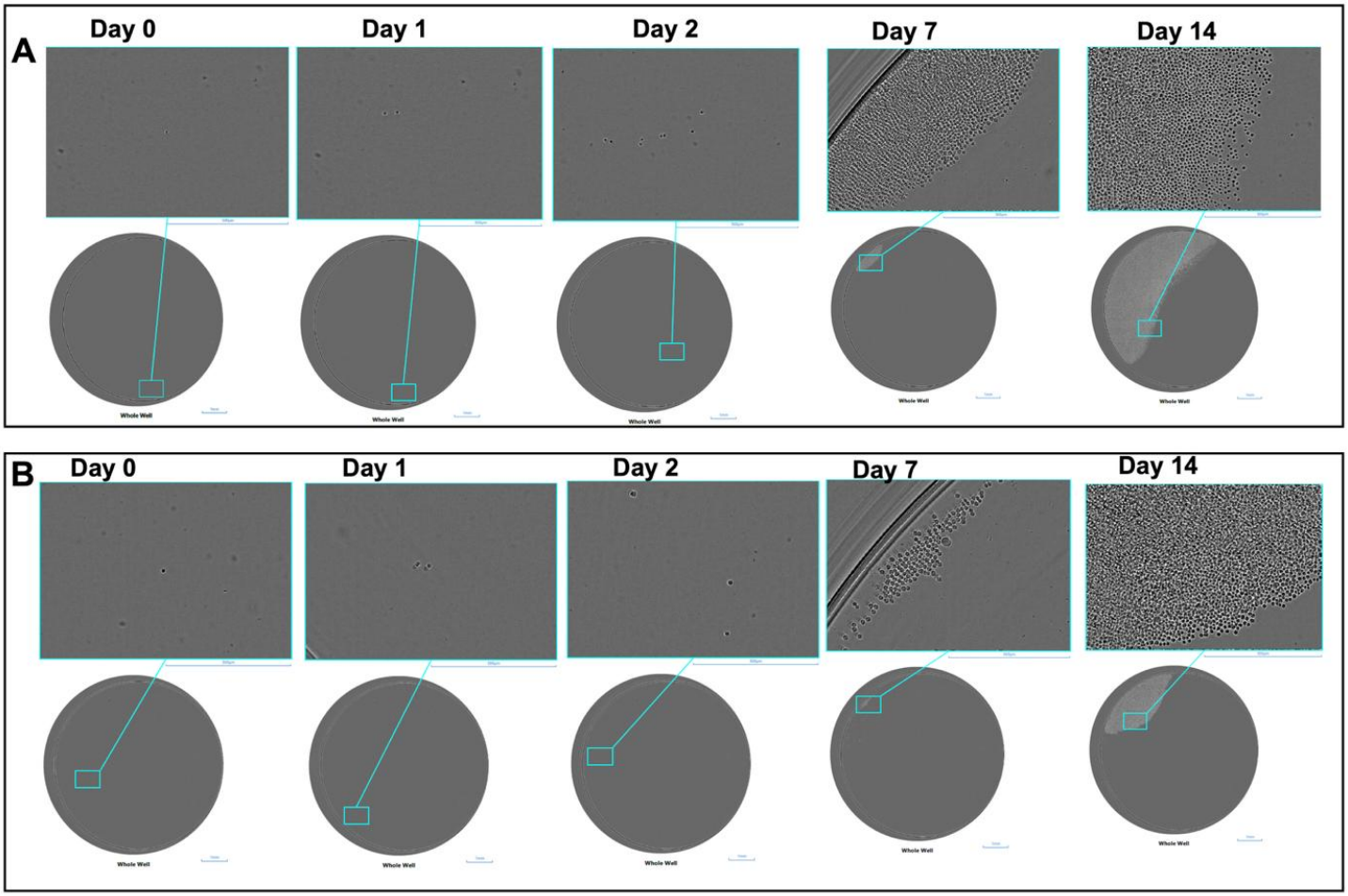

Figure 4 Solentim Images of P1B10 cell multiplication (**A**) and P2B9 cell multiplication (**B**).

Table 1 Yield and purity levels of rituximab from two best clones after Protein A chromatography

S. no.	Sample ID	Input volume (ml)	Input conc. (mg/ml)	Input volume (mL)	Output Conc. (mg/ml)	Output volume (ml)	Output Total IgG (mg)	Yield (%)	Purity by SEC-HPLC (%)
1	P1B10	19	1.09	20.71	4.923	4	19.692	95.084	92.5
2	P2B9	22	0.84	18.48	3.691	4	14.764	79.891	98

Physicochemical evaluation

Flores-Ortiz et al. has carried out extensive physicochemical analyses of the different commercially available Rituximab versions using RP- HPLC, Mass Spectrometry, SEC-MALS, CIEX chromatography, differential scanning calorimetry (DSC), hydrophobic interaction chromatography (HIC) and even potency assay **(Flores-Ortiz, Campos-García, Perdomo-Abúndez, Pérez, & Medina-Rivero, 2014)**. In the present study, we have carried out SEC-HPLC, CE-SDS, CIEX-HPLC and LC-MS analysis of the expressed Rituximab.

Size Exclusion Chromatography-High Performance Liquid Chromatography (SEC-HPLC)

High molecular-weight protein (HMWP) species, including aggregates, formed due to the association of two or more molecules of the antibody monomer. SEC-HPLC, in combination with ultraviolet (UV) detection, is used to resolve monomers and high molecular weight protein (HMWP) species present in Rituximab samples, as described in earlier studies **(Visser et al., 2013; Xu et al., 2019)**. The SEC-HPLC chromatograms of Rituximab from clarified harvests of P1B10 and P2B9 clones were analyzed to determine the relative content of monomer, HMWP species and low molecular weight protein (LMWP) species. The chromatogram overlays from SEC-HPLC analysis demonstrated the presence of HMWP and aggregates. The resolution of aggregates, the retention pattern of peaks was similar across both the samples evaluated (Figure 5). A higher percentage of LMWP species was observed in the P1B10 clone (Table 2).

Capillary Electrophoresis-Sodium Dodecyl sulphate (CE-SDS)

Capillary Electrophoresis-Sodium Dodecyl sulphate (CE-SDS) analysis was employed to determine the content of monomer and non-glycosylated heavy chain (Ng-HC). The non-reduced CE-SDS analysis was employed to assess the proportions of native monomers and the fragments, while the reduced CE-SDS analysis was used to quantify the Light Chain and Heavy Chain content, non-glycosylated Heavy Chain (Ng-HC), p75 variants (thio-ether impurity) and higher aggregated species **(Dada, Rao, Jones, Jaya, & Salas-Solano, 2017; Dadouch, Ladner, & Perrin, 2021; Visser et al., 2013; Xu et al., 2019)**.

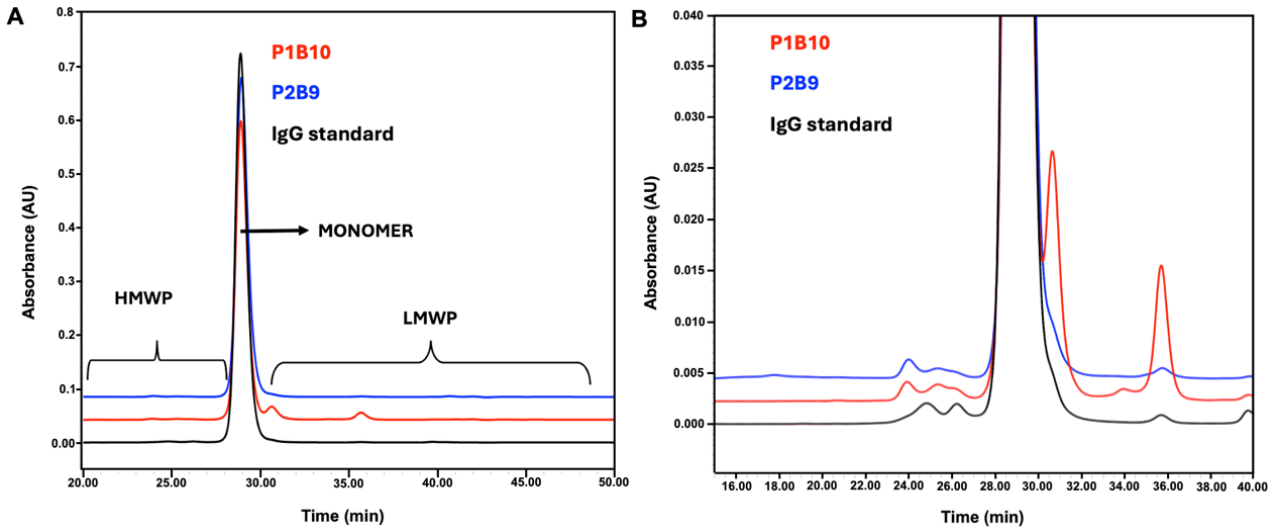

Figure 5 A) SEC-HPLC profiles of the clarified harvest of P1B10 and P2B9 of Rituximab *versus* immunoglobulin G (IgG) standard and B) zoomed SEC-HPLC profile.

Table 2 Percentage of size variants (as determine by SEC-HPLC) in clarified harvest batches P1B10 and P2B9 of Rituximab.

Sample Name	HMWP	MONOMER	LMWP
P1B10	0.88	92.45	6.66
P2B9	0.93	98.00	1.06

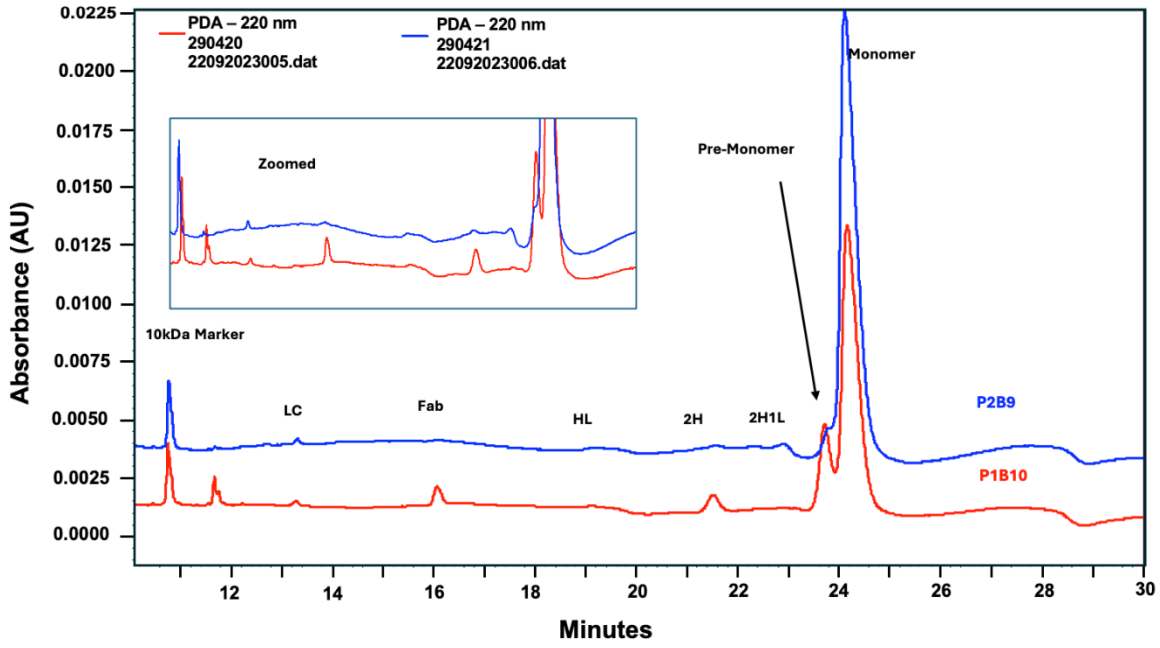

Figure 6 Non-Reduced CE-SDS profile overlay of Clarified harvest for the batch of P1B10 and P2B9 of Rituximab.

The non-reduced CE-SDS results corroborated SEC-HPLC results, i.e. higher LMWP species were observed in P1B10 in comparison to P2B9 clone (Figure 6, Table 3). The reduced CE-SDS results of P1B10 and P2B9 clones showed similar non-glycosylated heavy chain (Ng-HC) and p75 (a thio-ether impurity) variants free from LC and HC of the mAb. The representative reduced CE-SDS electropherogram profile overlays for P2B9 and P1B10 are presented in Figure 7. It was observed that P1B10 showed little higher fragments compared to the P2B9 clone (Table 4). The overall profile for the P2B9 clone seemed superior as compared to P1B10, making it a more preferred clone for further use.

Table 3 Percentage of monomer variants as determined by Non-Reduced CE-SDS data in the clarified harvest for the batch of P1B10 and P2B9 of Rituximab.

Sample Name	LC (%)	F_{ab} (%)	HL (%)	2H (%)	2H1L (%)	Pre-Monomer (%)	Monomer (%)	Total Impurity (%)
P1B10	0.62	3.07	0.47	3.38	ND	16.08	71.96	28.03
P2B9	0.55	0.22	0.10	0.38	1.13	3.25	93.98	6.02

Table 4 Percentage of fragments and Ng-HC as determined by Reduced CE-SDS data in the clarified harvest for the batch of P1B10 and P2B9 of Rituximab.

Sample Name	Fragment (%)	Fragment (%)	LC (%)	Fragment (%)	Fragment (%)	Fragment (%)	Fragment (%)	Ng-HC (%)	HC (%)	p75 (%)	LC+HC (%)	Total Impurity (%)
P1B10	1.97	0.45	34.47	1.41	1.27	0.65	4.15	0.95	54.55	0.12	89.02	10.97
P2B9	0.36	ND	34.82	ND	ND	ND	0.73	0.83	63.04	0.23	97.86	2.15

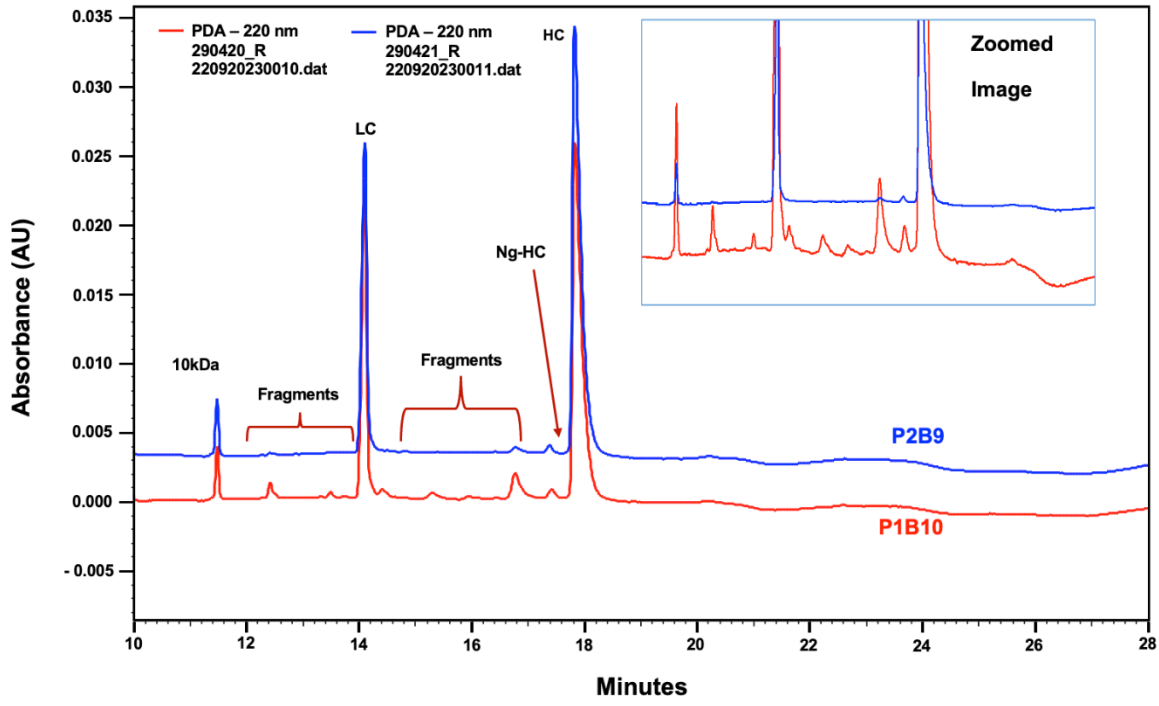

Figure 7 Reduced CE-SDS profile overlay of clarified harvest for the batch of P1B10 and P2B9 of Rituximab.

Table 5 Percentage of charge variants as determined by CIEX-UPLC the clarified harvest for the batch of P1B10 and P2B9 of Rituximab.

Sample Name	% Acidic	% Main Peak	% Basic
P1B10	17.13	46.14	36.72
P2B9	10.80	51.00	38.21

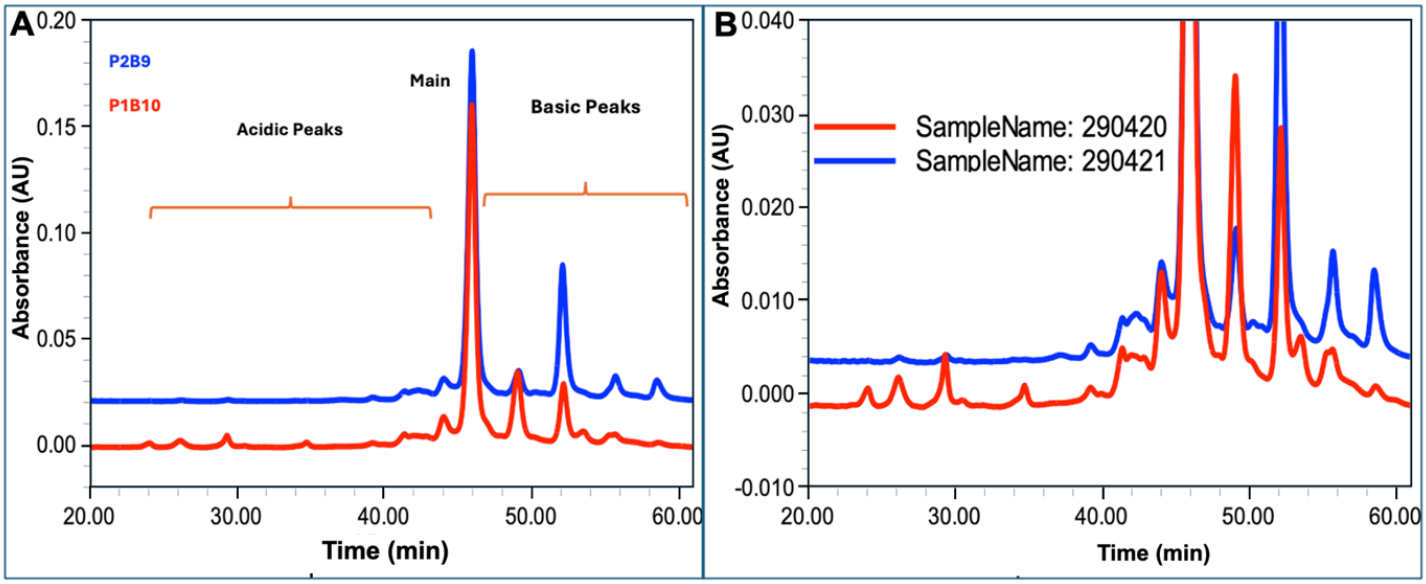

Figure 8 A) CIEX-HPLC profile overlay of the clarified harvest for the batch of P1B10 and P2B9 of Rituximab and B) zoomed CIEX-HPLC profile

Cation Exchange chromatography-High Performance Liquid Chromatography (CIEX-HPLC)

Cation Exchange chromatography is a form of ion exchange chromatography (IEX), which uses a negatively charged ion exchange resin with an affinity for molecules having net positive surface charges. As reported by earlier studies, the current study used cation exchange (CIEX)-HPLC to resolve variably charged species with minor charge differences **(Jing et al., 2020; Khawli et al., 2010; Luo et al., 2015)**. The predominant species is an unmodified variant that elutes as the main peak, whereas acidic variants elute earlier than the main peak and basic variants elute later than the main peak **(Jing et al., 2020)**. The distribution of variably charged species for Rituximab fed batch samples is shown in the representative chromatogram overlay of CIEX-HPLC (Figure 8, Table 5).

Higher main peaks and higher basic peaks were observed for P2B9 lots as compared to P1B10, whereas P1B10 clone has showed more acidic peaks. The acidic variants have been shown not to have any ill effects on the potency of the mAb (Flores-Ortiz et al., 2014). Higher basic peak in the P2B9 lots could be attributed to the manufacturing process. However, studies have reported that administration of similar mAbs has not shown any adverse effects or decrease in potency due to the presence of basic variants as the basic variants are usually excised at the C-terminal lysine residue in the bloodstream of the patient ~ 62 min after administration.

In view of this report, P2B9 clone seems to be a better candidate over P1B10. The intact mass analysis of the purified P1B10 and P2B9 samples are within 20 PPM of the Rituximab theoretical mass (Figure 9), thus confirming the identity of the purified samples.

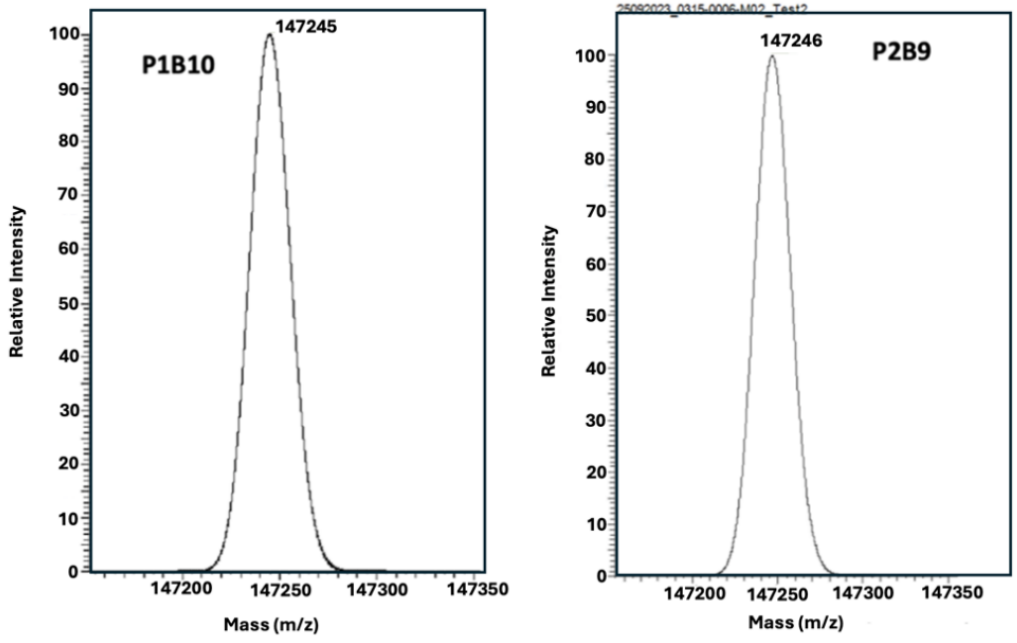

Figure 9 Intact mass Analysis - Deconvoluted mass spectra of (A) P1B10 and (B) P2B9 Rituximab.

CONCLUSIONS

The present study provides a stable clone for the expression of Rituximab using infusion cloning where two chains heavy chain (HC) and light chain (LC) are inserted together. High-yield clones, which is the prime goal of this work, were selected through accurate method that combined extensive data from clone selection and fed-batch cultures with orthogonal single-cell isolation techniques. From the 12 shortlisted clones, titer determination and viable cell density has allowed the selection of the 6 best clones, which were further narrowed down to 2 with fed-batch analysis. It was observed that the P1B10 clone produced a higher titer than the other clones. The Rituximab produced by the P2B9 clone had better size and charge variants profile as compared to the P1B10 clone. Thus, P2B9 was the clone of choice for future experiments including functional studies and large-scale production, which are on-going.

Acknowledgements: The authors express their gratitude to the Biocon Biologics Limited team and Dr. Anuj Goel for their constructive scientific inputs. Dr. Rajesh K P, Vaibhav, Sivaraj Dikeshwar Colon, and Dr. Nagaraj Govindappa are acknowledged for their invaluable support in facilitating the use of the Molecular Biology and Cell Culture Lab. Prasanthreddy L V and Karthick S are acknowledged for allowing us to utilize the Bioreactor for this study. Koduru Srivatsa, Dr. Chethan G H and Navratna P are acknowledged for granting access to the characterization facility.

REFERENCES

Aoyama, S., Matsumoto, Y., Mori, C., & Sota, K. (2022). Application of novel mixed mode chromatography (MMC) resins having a hydrophobic modified polyallylamine ligand for monoclonal antibody purification. *Journal of Chromatography B*, *1191*, 123072. doi: 10.1016/j.jchromb.2021.123072

Bennett, C., Qureshi, Z., Singh, & Magwood, J. (2013). Rituximab and biosimilars—Equivalence and reciprocity. *Biosimilars*, 19. doi: 10.2147/BS.S20681

Bolisetty, P., Tremml, G., Xu, S., & Khetan, A. (2020). Enabling speed to clinic for monoclonal antibody programs using a pool of clones for IND-enabling toxicity studies. *mAbs*, *12*(1), 1763727. doi: 10.1080/19420862.2020.1763727

Buss, N. A., Henderson, S. J., McFarlane, M., Shenton, J. M., & De Haan, L. (2012). Monoclonal antibody therapeutics: History and future. *Current Opinion in Pharmacology*, *12*(5), 615–622. doi: 10.1016/j.coph.2012.08.001

Coiffier, B. (2017). Pharmacokinetics, efficacy and safety of the rituximab biosimilar CT-P10. *Expert Review of Clinical Pharmacology*, *10*(9), 923–933. doi: 10.1080/17512433.2017.1359537

Dada, O. O., Rao, R., Jones, N., Jaya, N., & Salas-Solano, O. (2017). Comparison of SEC and CE-SDS methods for monitoring hinge fragmentation in IgG1 monoclonal antibodies. *Journal of Pharmaceutical and Biomedical Analysis*, *145*, 91–97. doi: 10.1016/j.jpba.2017.06.006

Dadouch, M., Ladner, Y., & Perrin, C. (2021). Analysis of Monoclonal Antibodies by Capillary Electrophoresis: Sample Preparation, Separation, and Detection. *Separations*, *8*(1), 4. doi: 10.3390/separations8010004

Du, F. H., Mills, E. A., & Mao-Draayer, Y. (2017). Next-generation anti-CD20 monoclonal antibodies in autoimmune disease treatment. *Autoimmunity Highlights*, *8*(1), 12. doi: 10.1007/s13317-017-0100-y

Falzone, L., Salomone, S., & Libra, M. (2018). Evolution of Cancer Pharmacological Treatments at the Turn of the Third Millennium. *Frontiers in Pharmacology*, *9*, 1300. doi: 10.3389/fphar.2018.01300

Flores-Ortiz, L. F., Campos-García, V. R., Perdomo-Abúndez, F. C., Pérez, N. O., & Medina-Rivero, E. (2014). PHYSICOCHEMICAL PROPERTIES OF RITUXIMAB. *Journal of Liquid Chromatography & Related Technologies*, *37*(10), 1438–1452. doi: 10.1080/10826076.2013.794738

Grillo-López, A. J. (2005). Rituximab: Clinical Development of the First Therapeutic Antibody for Cancer. In O. Kayser & R. H. Müller (Eds.), *Pharmaceutical Biotechnology* (pp. 211–229). Weinheim, FRG: Wiley-VCH Verlag GmbH & Co. KGaA. doi: 10.1002/3527602410.ch12

Gross, T., Jeney, C., Halm, D., Finkenzeller, G., Stark, G. B., Zengerle, R., … Zimmermann, S. (2021). Characterization of CRISPR/Cas9 RANKL knockout mesenchymal stem cell clones based on single-cell printing technology and Emulsion Coupling assay as a low-cellularity workflow for single-cell cloning. *PLOS ONE*, *16*(3), e0238330. doi: 10.1371/journal.pone.0238330

Jin, S., Sun, Y., Liang, X., Gu, X., Ning, J., Xu, Y., … Pan, L. (2022). Emerging new therapeutic antibody derivatives for cancer treatment. *Signal Transduction and Targeted Therapy*, *7*(1), 39. doi: 10.1038/s41392-021-00868-x

Jing, S.-Y., Gou, J.-X., Gao, D., Wang, H.-B., Yao, S.-J., & Lin, D.-Q. (2020). Separation of monoclonal antibody charge variants using cation exchange chromatography: Resins and separation conditions optimization. *Separation and Purification Technology*, *235*, 116136. doi: 10.1016/j.seppur.2019.116136

Kaplon, H., & Reichert, J. M. (2021). Antibodies to watch in 2021. *mAbs*, *13*(1), 1860476. doi: 10.1080/19420862.2020.1860476

Khawli, L. A., Goswami, S., Hutchinson, R., Kwong, Z. W., Yang, J., Wang, X., … Motchnik, P. (2010). Charge variants in IgG1: Isolation, characterization, in vitro binding properties and pharmacokinetics in rats. *mAbs*, *2*(6), 613–624. doi: 10.4161/mabs.2.6.13333

Köhler, G., & Milstein, C. (1975). Continuous cultures of fused cells secreting antibody of predefined specificity. *Nature*, *256*(5517), 495–497. doi: 10.1038/256495a0

Li, R., Dowd, V., Stewart, D. J., Burton, S. J., & Lowe, C. R. (1998). Design, synthesis, and application of a Protein A mimetic. *Nature Biotechnology*, *16*(2), 190–195. doi: 10.1038/nbt0298-190

Lin, M. J., Svensson-Arvelund, J., Lubitz, G. S., Marabelle, A., Melero, I., Brown, B. D., & Brody, J. D. (2022). Cancer vaccines: The next immunotherapy frontier. *Nature Cancer*, *3*(8), 911–926. doi: 10.1038/s43018-022-00418-6

Longo, P. A., Kavran, J. M., Kim, M.-S., & Leahy, D. J. (2014). Single Cell Cloning of a Stable Mammalian Cell Line. In *Methods in Enzymology* (Vol. 536, pp. 165–172). Elsevier. doi: 10.1016/B978-0-12-420070-8.00014-3

Lu, R.-M., Hwang, Y.-C., Liu, I.-J., Lee, C.-C., Tsai, H.-Z., Li, H.-J., & Wu, H.-C. (2020). Development of therapeutic antibodies for the treatment of diseases. *Journal of Biomedical Science*, *27*(1), 1. doi: 10.1186/s12929-019-0592-z

Luo, H., Cao, M., Newell, K., Afdahl, C., Wang, J., Wang, W. K., & Li, Y. (2015). Double-peak elution profile of a monoclonal antibody in cation exchange chromatography is caused by histidine-protonation-based charge variants. *Journal of Chromatography A*, *1424*, 92–101. doi: 10.1016/j.chroma.2015.11.008

Maloney, D. G., Grillo-López, A. J., White, C. A., Bodkin, D., Schilder, R. J., Neidhart, J. A., … Levy, R. (1997). IDEC-C2B8 (Rituximab) Anti-CD20 Monoclonal Antibody Therapy in Patients With Relapsed Low-Grade Non-Hodgkin's Lymphoma. *Blood*, *90*(6), 2188–2195. doi: 10.1182/blood.V90.6.2188

Margoni, M., Preziosa, P., Filippi, M., & Rocca, M. A. (2022). Anti-CD20 therapies for multiple sclerosis: Current status and future perspectives. *Journal of Neurology*, *269*(3), 1316–1334. doi: 10.1007/s00415-021-10744-x

Mishra, R., Singh, V., & Pritchard, C. H. (2011). Safety of biologic agents after rituximab therapy in patients with rheumatoid arthritis. *Rheumatology International*, *31*(4), 481–484. doi: 10.1007/s00296-009-1307-7

Noy-Porat, T., Alcalay, R., Mechaly, A., Peretz, E., Makdasi, E., Rosenfeld, R., & Mazor, O. (2021). Characterization of antibody-antigen interactions using biolayer interferometry. *STAR Protocols*, *2*(4), 100836. doi: 10.1016/j.xpro.2021.100836

Passariello, M., Esposito, S., Manna, L., Rapuano Lembo, R., Zollo, I., Sasso, E., … De Lorenzo, C. (2023). Comparative Analysis of a Human Neutralizing mAb Specific for SARS-CoV-2 Spike-RBD with Cilgavimab and Tixagevimab for the Efficacy on the Omicron Variant in Neutralizing and Detection Assays. *International Journal of Molecular Sciences*, *24*(12), 10053. doi: 10.3390/ijms241210053

Pierpont, T. M., Limper, C. B., & Richards, K. L. (2018). Past, Present, and Future of Rituximab—The World's First Oncology Monoclonal Antibody Therapy. *Frontiers in Oncology*, *8*, 163. doi: 10.3389/fonc.2018.00163

Riba, J., Schoendube, J., Zimmermann, S., Koltay, P., & Zengerle, R. (2020). Single-cell dispensing and 'real-time' cell classification using convolutional neural networks for higher efficiency in single-cell cloning. *Scientific Reports*, *10*(1), 1193. doi: 10.1038/s41598-020-57900-3

Ryu, J., Kim, E.-J., Kim, J.-K., Park, T. H., Kim, B.-G., & Jeong, H.-J. (2022). Development of a CHO cell line for stable production of recombinant antibodies against human MMP9. *BMC Biotechnology*, *22*(1), 8. doi: 10.1186/s12896-022-00738-6

Scherzinger, J., Türk, D., & Aprile-Garcia, F. (2022). *An optimized and validated workflow for developing stable producer cell lines with >99.99% assurance of clonality and high clone recovery* [Preprint]. Bioengineering. doi: 10.1101/2022.12.16.520697

Sellebjerg, F., Blinkenberg, M., & Sorensen, P. S. (2020). Anti-CD20 Monoclonal Antibodies for Relapsing and Progressive Multiple Sclerosis. *CNS Drugs*, *34*(3), 269–280. doi: 10.1007/s40263-020-00704-w

Sharman, J. P., Liberati, A. M., Ishizawa, K., Khan, T., Robbins, J., Alcasid, A., … Aurer, I. (2020). A Randomized, Double-Blind, Efficacy and Safety Study of PF-05280586 (a Rituximab Biosimilar) Compared with Rituximab Reference Product (MabThera®) in Subjects with Previously Untreated CD20-Positive, Low-Tumor-Burden Follicular Lymphoma (LTB-FL). *BioDrugs*, *34*(2), 171–181. doi: 10.1007/s40259-019-00398-7

Shukla, P. K., Radmall, K. S., & Chandrasekharan, M. B. (2023). Rapid purification of rabbit immunoglobulins using a single-step, negative-selection chromatography. *Protein Expression and Purification*, *207*, 106270. doi: 10.1016/j.pep.2023.106270

Singh, S., Kumar, N. K., Dwiwedi, P., Charan, J., Kaur, R., Sidhu, P., & Chugh, V. K. (2018a). Monoclonal Antibodies: A Review. *Current Clinical Pharmacology*, *13*(2), 85–99. doi: 10.2174/1574884712666170809124728

Singh, S., Kumar, N. K., Dwiwedi, P., Charan, J., Kaur, R., Sidhu, P., & Chugh, V. K. (2018b). Monoclonal Antibodies: A Review. *Current Clinical Pharmacology*, *13*(2), 85–99. doi: 10.2174/1574884712666170809124728

Swartz, A. R., & Chen, W. (2018). Rapid Quantification of Monoclonal Antibody Titer in Cell Culture Harvests by Antibody-Induced Z-ELP-E2 Nanoparticle Cross-Linking. *Analytical Chemistry*, *90*(24), 14447–14452. doi: 10.1021/acs.analchem.8b04083

Todd, P. A., & Brogden, R. N. (1989). Muromonab CD3: A Review of its Pharmacology and Therapeutic Potential. *Drugs*, *37*(6), 871–899. doi: 10.2165/00003495-198937060-00004

Vallone, V. F., Telugu, N. S., Fischer, I., Miller, D., Schommer, S., Diecke, S., & Stachelscheid, H. (2020). Methods for Automated Single Cell Isolation and Sub-Cloning of Human Pluripotent Stem Cells. *Current Protocols in Stem Cell Biology*, *55*(1), e123. doi: 10.1002/cpsc.123

Visser, J., Feuerstein, I., Stangler, T., Schmiederer, T., Fritsch, C., & Schiestl, M. (2013). Physicochemical and Functional Comparability Between the Proposed Biosimilar Rituximab GP2013 and Originator Rituximab. *BioDrugs*, *27*(5), 495–507. doi: 10.1007/s40259-013-0036-3

Walsh, G., & Walsh, E. (2022). Biopharmaceutical benchmarks 2022. *Nature Biotechnology*, *40*(12), 1722–1760. doi: 10.1038/s41587-022-01582-x

World Health Organization. (2020). *WHO report on cancer: Setting priorities, investing wisely and providing care for all*. Geneva: World Health Organization. Retrieved from https://apps.who.int/iris/handle/10665/330745

Xu, Y., Xie, L., Zhang, E., Gao, W., Wang, L., Cao, Y., … Liu, S. (2019). Physicochemical and functional assessments demonstrating analytical similarity between rituximab biosimilar HLX01 and the MabThera®. *mAbs*, *11*(3), 606–620. doi: 10.1080/19420862.2019.1578147

Yang, W., Zhang, J., Xiao, Y., Li, W., & Wang, T. (2022). Screening Strategies for High-Yield Chinese Hamster Ovary Cell Clones. *Frontiers in Bioengineering and Biotechnology*, *10*, 858478. doi: 10.3389/fbioe.2022.858478

Yeh, C.-F., Lin, C.-H., Chang, H.-C., Tang, C.-Y., Lai, P.-T., & Hsu, C.-H. (2020). A Microfluidic Single-Cell Cloning (SCC) Device for the Generation of Monoclonal Cells. *Cells*, *9*(6), 1482. doi: 10.3390/cells9061482

Zitzmann, J., Schreiber, C., Eichmann, J., Bilz, R. O., Salzig, D., Weidner, T., & Czermak, P. (2018). Single-cell cloning enables the selection of more productive Drosophila melanogaster S2 cells for recombinant protein expression. *Biotechnology Reports*, *19*, e00272. doi: 10.1016/j.btre.2018.e00272

Supplementary information

Table S1 Sequences of the primers used for amplification of Lc and Hc of Rituximab

Sr. No.	Primer Name	Primer Sequence (5'→ 3')	Target gene
1.	Rituximab_pCHO 1.0_LC1 (forward)	GAGCTCAAGCTTGATATCGCCACCATGATGTCTTTTGTGTC	Lc
2.	Rituximab_pCHO 1.0_LC2 (reverse)	CTGGATCGAAGCTTAATTAATTACTATCAGCACTCGCCCCG	
3.	Rituximab_pCHO 1.0_HC1 (forward)	TTCCGGGCCGCCTAGGGCCACCATGATGTCTTTTGTGTC	Hc
4.	Rituximab_pCHO 1.0_HC2 (reverse)	GTATAATATAGAGTATACTTACTATCACTTGCCAGGGGACAG	

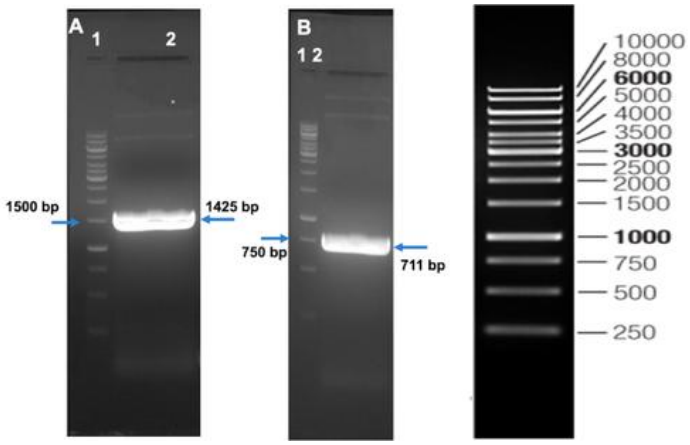

Figure S1 Agarose Gel Electrophoresis of PCR products. The PCR products of Rituximab Lc and Hc were run on 0.8% agarose gel to check for the sizes and subsequent gel elution for further cloning process. **(A) Lane 1:** GeneRuler 1kb DNA Ladder; **Lane 2:** Rituximab Hc PCR product (1425 bp) running just below 1500 bp band. **(B) Lane 1:** GeneRuler 1kb DNA Ladder; **Lane 2:** Rituximab Lc PCR product (711 bp) running just below 750 bp band.

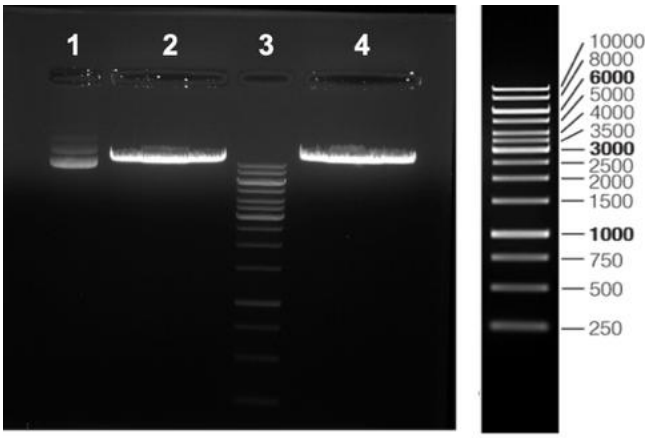

Figure S2 Agarose Gel Electrophoresis of EcoRV and PacI digested pCHO 1.0 vector. The digested pCHO 1.0 vector was run on 0.8% agarose gel to check for the presence of single band (Lanes 2 and 4). The band was then eluted and used for downstream cloning procedure. Undigested pCHO 1.0 vector was loaded as a control (Lane 1) and the GeneRuler 1 kb DNA ladder worked as the marker (Lane 3).

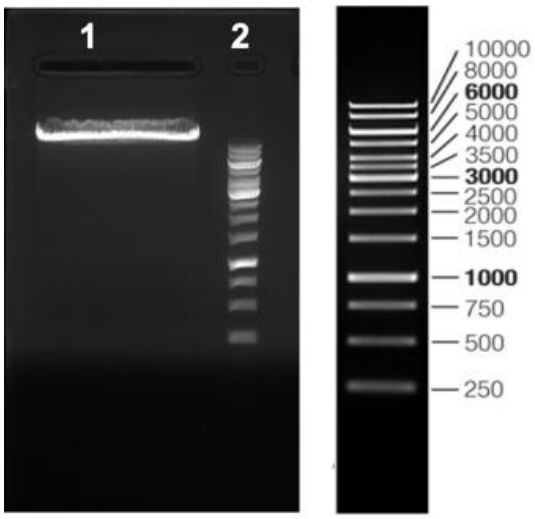

Figure S3 Agarose Gel Electrophoresis of AvrII and BstZ17I digested pCHO 1.0 + Lc plasmid. The digested pCHO 1.0 + Lc plasmid was run on 0.8% agarose gel to check for the presence of single band (Lane 1). The band was then eluted and used for downstream cloning procedure. GeneRuler 1 kb DNA ladder worked as the size marker (Lane 2).

Table S2 Restriction digestion pattern for clone confirmation of pCHO 1.0+Lc+Hc plasmid from clones 1 and 3.

Enzyme combination	Recombinant (pCHO 1.0+Lc+Hc)			Native Plasmid (pCHO 1.0)		
	Total (bp)	Fragment -1 (bp)	Fragment -2 (bp)	Total (bp)	Fragment -1 (bp)	Fragment -2 (bp)
AvrII + BstZ17I	15117	1433	13684	12988	Linearization (12988)	
BstZ17I + PacI		2777	12340		2070	10918
NruI		Linearization (15117)			Linearization (12988)	
EcoRI		1156	13961		Linearization (12988)	
KpnI + AvrII		8924	6193		8924	4064

Table S3 Selection scheme for the two phases of selection. TF denote Rituximab transfected flask while F in flask ID denotes the shake flasks used for selection of stable cell pools. P denotes Puromycin and M denotes Methotraxate. 10P/100M stands for 10 µg/mL Puromycin and 100 nM Methotrexate. 20P/200M stands for 20 µg/mL Puromycin and 200 nM Methotrexate. 30P/500M stands for 30 µg/mL Puromycin and 500 nM Methotrexate. 50P/1000M stands for 50 µg/mL Puromycin and 1000 nM Methotrexate.

Flask ID	Source Flaks	Phase-1 selection pressure	Phase-2 selection pressure	Viability (%)	Calculated Concentration (µg/mL)
F1	TF1	10P/100M	30P/500M	93	19.4
F2	TF2	10P/100M	30P/500M	95	14.8
F3	TF1	20P/200M	30P/500M	97	18.4
F4	TF2	20P/200M	30P/500M	98	16.6
F5	TF1	10P/100M	50P/1000M	90	7.31
F6	TF2	10P/100M	50P/1000M	91	7.99
F7	TF1	20P/200M	50P/1000M	90	11.5
F8	TF2	20P/200M	50P/1000M	94	14.5

Table S4 VCD, % viability and Rituximab titers during the period of Fed-Batch analysis. Octet analysis was not done on Day 0, Days 12 and 13.

Flask ID	Titer (µg/mL)					
	Day 3	Day 5	Day 7	Day 9	Day 11	Day 14
F1	66	143	267	463.1	652.1	1094.4
F2	59	148	295	521.3	778.6	1291.9
F3	76	161	333	537.6	853.7	1329.1
F4	66	152	287	478.9	764.6	1189.3
F5	36	124	273	555.8	731.6	1096.8
F6	42	131	286	528.4	821.5	**1440.2**
F7	64	162	333	544.6	905.3	1316.9
F8	61	158	318	539.5	711.9	1234.4

Table S5 Rituximab titers during the period of Fed-Batch analyses of the single cell clones sorted using Cyetna F.Sight™. Each Sample ID depict the plate number (P1, P2 or P3) and well number (A1-A12, B1-B12, C1-C12, D1-D12, E1-E12, F1-F12, G1-G12 or H1-H12) for the single cell clone sorted into 3 different 96-well plates.

	Rituximab Titer (µg/mL)				
Sample ID	**Day 5**	**Day 7**	**Day 9**	**Day 11**	**Day 13**
P1B6	**154.3**	**355.4**	**591.1**	**717**	**658.1**
P1B10	**172.8**	**419.3**	**696.1**	**827.9**	**1059.2**
P1D2	83	187.4	331.8	450.1	418.6
P1D11	102.5	213.8	337.4	431.2	409
P1G2	**127.3**	**276.5**	**452.1**	**544.2**	**507.3**
P2B5	**141.5**	**332.7**	**547.8**	**656.1**	**680.2**
P2B9	**154**	**359.2**	**595.4**	**703.9**	**695.3**
P2F7	109.4	227.4	384.3	531.8	504.6
P2G8	125.3	233.2	329.4	401.8	487.8
P3D7	159.1	301	499.6	554.4	515.7
P3E10	**144.6**	**319.9**	**429.1**	**607.7**	**545.3**
P3F4	125.6	282.9	440.7	494.9	488.4

Table S6 Shortlisted clones

Sample ID	Lot	Day-5	Day-7	Day-9	Day-11	Day-14
P1B6	1A	105.2	371.1	557.6	643	841.9
	1B	115.8	367.8	524.3	734.9	852.5
P1B10	2A	174.9	255.8	838.7	1014.9	1154.3
	2B	153.8	255.8	904.8	1021.3	1219.2
P1G2	3A	74.4	174.7	330	413.4	535.3
	3B	73.5	173.8	334.6	405.5	524.6
P2B5	4A	102.1	240.8	561.8	620.1	713.9
	4B	105.1	244	525.4	719.4	808.3
P2B9	5A	139.6	328.6	674.6	797.5	887.8
	5B	154.1	326.2	625.1	772.1	908.9
P3E10	6A	147.1	266.4	506.4	599.4	739.9
	6B	134.0	272.1	529.7	644	892.7